208. Acyl Migration in d^6 Iron Complexes

by **Pius Kölbener, Hans-Ulrich Hund, H. William Bosch, Christoph Sontag,** and **Heinz Berke***

Anorganisch-chemisches Institut der Universität Zürich, Winterthurerstr. 190, CH-8057 Zürich

(11.X.90)

The η^2-acyl complex [Fe(η^2-EtC=O)I (CO)(PEt_3)$_2$] (**1a**) reacts with phenylacetylene in refluxing Et_2O to form a mixture of products including [Fe{C(Ph)=CHC(O)Et}I(CO)(PEt_3)$_2$] (**3**), [Fe{C(Ph)=CHC(O)Et}I(CO)$_2$(PEt_3)$_2$] (**4**), and [Fe{C(=CHPh)C(O)Et}I(CO)(PEt_3)$_2$] (**5**). Compound **3** contains a 'metallafurane' unit, while **5** consists of a 4-member metallacycle. Compound **5** was characterized by X-ray crystallography. In contrast to **1a**, the η^2-acyl complex [Fe{η^2-(i-Pr)CO}I(CO)(PEt_3)$_2$] (**1b**) reacts with phenylacetylene under similar conditions to produce [Fe{η^2-C(O)C(Ph)=CH(i-Pr)}I(CO)(PEt_3)$_2$ (**7**) which was characterized spectroscopically. Modified extended *Hückel* theory calculations were made on the model compounds [Fe(η^2-CHO)(CO)$_2$(PH_3)$_2$]$^+$ (**14**), [Fe(CHO)(HCCH)(CO)$_2$(PH_3)$_2$]$^+$ (**15**), [Fe(=C=CH$_2$)(CHO)(CO)$_2$(PH_3)$_2$]$^+$ (**16**), [Fe{C(=CH$_2$)CHO}(CO)$_2$(PH_3)$_2$]$^+$ (**17**), and {Fe(CH=CHCHO)(CO)$_2$(PH_3)$_2$]$^+$ (**18**). The calculations show that in the transformation **15**→**18**, there exists a transition state lying 83.6 kJ/mol above the optimized geometry of **15** in which the formyl unit is rotated by 80° with respect to the Fe-acetylene plane. Conversion of **15** to **17** involves a [1,2]-H shift and an acyl-acetylene coupling reaction which probably occur synchronously.

Transition metal bound acyl and acetylene units can undergo facile coupling reactions to yield enone complexes. Such C–C bond forming processes have been found to occur at manganese [1], group VIb transition metal [2], ruthenium [3], and nickel centers [4] and are applicable to syntheses of natural products [4]. It was expected that further variation of the transition-metal fragment would bring about new ways of combining acyl and acetylenic units.

In earlier papers, we have described the synthesis of (η^2-acyl)carbonyliodobis-(phosphorus donor)iron complexes, which can easily provide an empty coordination site [5] [6]. The addition of an acetylene molecule would lead to (acyl)(acetylene) complexes as precursors for the desired reactivity.

Results and Discussion. – As indicated in *Scheme 1*, the carbonyliodo(propionyl)-bis(triethylphosphine)iron complex **1a** reacts with phenylacetylene under reflux in Et_2O to yield four isolable compounds, *i.e.* the insertion products into the Fe–acyl bond **3**–**5** and the known CO-addition product **6a** [6]. The isolation of **3**–**5** was rather difficult. Separation was finally achieved by several chromatographic operations in combination with solvent extractions. The compounds were identified spectroscopically (see *Table 1*) and by elemental analyses. An X-ray structure analysis was carried out on **5** which confirmed the spectroscopically derived constitution.

It can be assumed that the intermediate appearance of an acyl(phenylacetylene) complex **2** is followed by a coupling reaction of both ligand units to generate the red brown 'ferrafurane' derivative **3**. Under the reaction conditions applied, **3** is subsequently transformed to **4** by uptake of a CO molecule. For the formation of the dark blue carbonyliodo(3-oxo-1-phenylpent-1-en-2-yl)bis(triethylphosphine)iron **5**, it is reasonable

Scheme 1

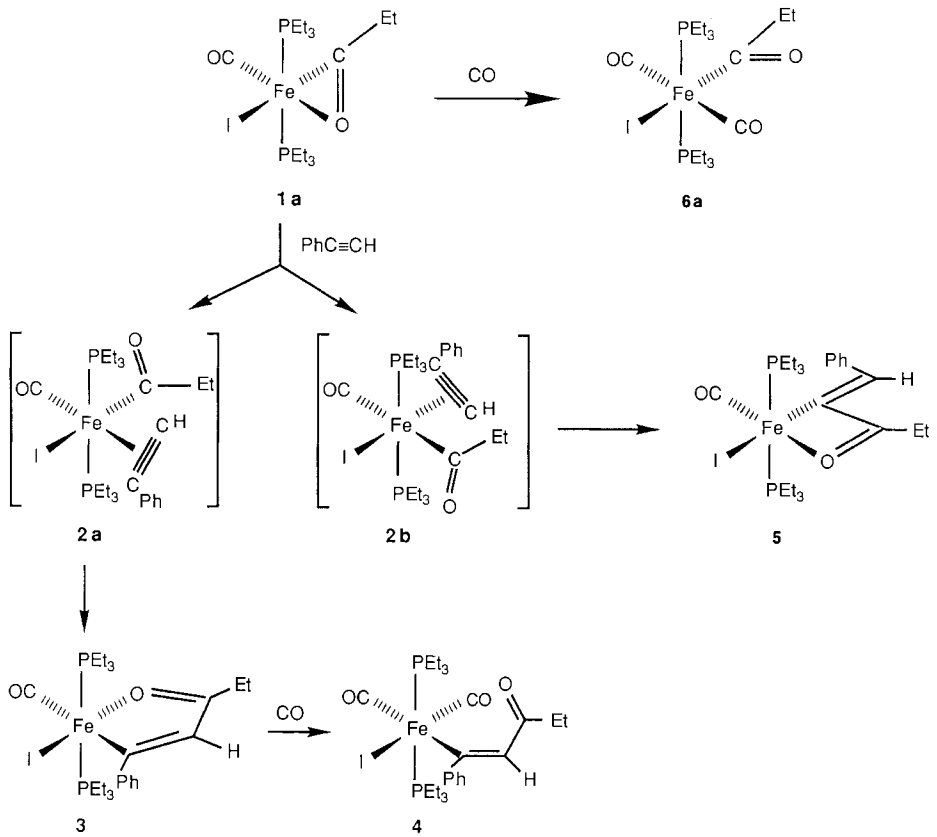

to anticipate a sequence of two elementary steps starting from **2**. The reaction could proceed through an acetylene/vinylidene rearrangement followed by a 1,2 shift of the propionyl onto the vinylidene group to generate **5**. There is some indication, especially from the theoretical investigations (see below), that the migration of the H-atom and the acyl moiety take place simultaneously. Attempts to replace the Fe-bound O-atom in **5** by a CO ligand were unsuccessful, even if elevated CO pressures were applied. Obviously, this is due to the entropic contribution of the chelate effect of the 1-propionylvinyl group rather than the strength of the Fe–O bond.

The spectroscopic data of **3** show that the PEt_3 groups are in *trans* positions. Insertion of the phenylacetylene molecule occurs regioselectively so that the Ph substituent is bound at C(1) of the new ligand. A $^1H,^1H$ COSY experiment confirmed that the coupling of the olefinic proton (2.6 Hz, see *Table 1*) is not the result of an H,H interaction and, therefore, must be due to an H,P interaction. The magnitude of this coupling is consistent with the olefinic proton being in β-position with respect to the metal center; coupling to a C*H*(α) would be expected in the range 6–7 Hz. The COSY experiment with **3** also showed that, as in the case of **4**, there is coupling to the Ph protons (1.3 Hz) which must due to the P-nuclei and can only be anticipated for Ph substituents attached at C(α) of the metallacycle. The assignment of the position of the O-substituent *trans* to the I-ligand was based on the assumption that **4** is a CO substitution product of **3** and the CO ligand replaces the O-atom of the acyl ligand in this compound. Since the ^{13}C-NMR and IR spectra of **4** made clear that it contains two chemically inequivalent CO groups in

Table 1. *^{1}H-NMR, ^{13}C-NMR, and IR Spectroscopic Data of Compounds* **3**–**5** *and* **7**[a])

	^{1}H-NMR	^{13}C-NMR	IR
3	8.16 (*t*, *J* = 2.6, C=CH); 7.64 (*d*, *J* = 7.7, 2 H_o); 7.36 (*t*, *J* = 7.7, 2 H_m); 7.20 (*t*, *J* = 7.7, 1 H_p); 3.61 (*q*, *J* = 7.7, CH_3CH_2CO); 1.76 (*m*, 2 $(CH_3CH_2)_3P$); 1.28 (*t*, *J* = 7.7, CH_3CH_2CO); 1.00 (*m*, 2 $(CH_3CH_2)_3P$)	229.7 (*t*, *J* = 29.5, C≡O); 213.2 (*t*, *J* = 17.3, C=O); 156.2 (*t*, *J* = 6.8, Fe–C=*C*); 151.9 (*t*, *J* = 32.7, Fe–*C*=C); 132.6 (*s*, Ph); 128.9 (*s*, Ph); 126.2 (*s*, Ph); 123.3 (*s*, Ph); 49.0 (*s*, CH_3CH_2CO); 19.4 (*t*, *J* = 13.1, $(CH_3CH_2)_3P$); 10.8 (*s*, CH_3CH_2CO); 8.2 (*s*, $(CH_3CH_2)_3P$)	1943*s*, 1603*w*
4	7.91 (*d*, *J* = 7.6, 2 H_o); 7.36 (*t*, *J* = 7.6, 2 H_m, H_p); 7.25 (*t*, *J* = 1.4, C=CH); 2,92 (*q*, *J* = 7.4, CH_3CH_2CO); 1.34 (*m*, $(CH_3CH_2)_3P$); 1.18 (*t*, CH_3CH_2CO); 0.95 (*m*, 2 $(CH_3CH_2)_3P$)	222.9 (*t*, *J* = 26.8, C≡O); 221.9 (*t*, *J* = 26.8, C=O); 197.3 (*t*, Fe–*C*=C); 134.9 (*s*, Fe–C=*C*); 128.5 (*m*, Ph); 37.7 (*s*, CH_3CH_2CO); 18.2 (*t*, *J* = 10.9, $(CH_3CH_2)_3P$); 9.3 (*s*, CH_3CH_2CO); 7.3 (*s*, $(CH_3CH_2)_3P$)	1955*s*, 1888*s*, 1635*w*
5	8.62 (*t*, *J* = 4.0, C=CH); 7.85 (*m*, 2 H, Ph); 7.38 (*m*, 3 H, Ph); 2.82 (*q*, *J* = 7.4, CH_3CH_2CO); 1.93 (*m*, 2 $(CH_3CH_2)_3P$); 1.3–1.00 (*m*, 2 $(CH_3CH_2)_3P$, CH_3CH_2CO)	225.4 (*t*, *J* = 31.4, C≡O); 223.0 (*s*, C=O); 161.6 (*t*, *J* = 22.1, Fe–*C*=C); 155.8 (*s*, Fe–C=*C*); 138.2 (*s*, Ph); 129.1 (*s*, Ph); 128.5 (*s*, Ph); 128.3 (*s*, Ph); 29.0 (*s*, CH_3CH_2CO); 17.5 (*t*, *J* = 11.3, $CH_3CH_2)_3P$); 7.7 (*s*, CH_3CH_2CO); 6.7 (*s*, $(CH_3CH_2)_3P$)	1910*s* (br.), 1902 (sh), 1546*w*
7	7.4–7.0 (*m*, Ph); 7.34 (*d*, *J* = 10.7, C=CH); 2.72 (*sept. d*, *J* = 10.7, 6.6, $(CH_3)_2CH$); 1.89 (*m*, 2 $(CH_3CH_2)_3P$); 1.12 (*d*, *J* = 6.6, $(CH_3)_2CH$); 1.03 (*m*, 2 $(CH_3CH_2)_3P$)	270.9 (*t*, *J* = 34.5, C=O); 224.1 (*t*, *J* = 20.0, C≡O); 164.3 (*s*, CH=CCO); 136.7 (*t*, *J* = 2.3, CH=*C*CO); 135–127 (*m*, Ph); 29.0 (*s*, $(CH_3)_2CH$); 21.0 (*s*, $(CH_3)_2CH$); 18.0 (*t*, *J* = 11.9, $(CH_3CH_2)_3P$); 8.10 (*t*, *J* = 1.3, $(CH_3CH_2)_3P$)	1891*s*

[a]) ^{1}H- and ^{13}C-NMR in $CDCl_3$ δ in ppm; *J*(H,H) and *J*(P,H) in Hz. IR: in hexane (**3**, **4**, and **7**) or $CHCl_3$ (**5**).

cis-position, one can conclude that in **3**, the I- and O-substituent have to be *trans* to each other. The metallacyclic arrangement of the enone unit in **3** causes significant differences of the chemical shifts of corresponding proton resonances in comparison to **4**. The olefinic proton of **3** is shifted by nearly 1 ppm to lower field, probably induced by a ring-current effect in the 'metallafuran' system (see *Table 1*).

Scheme 2

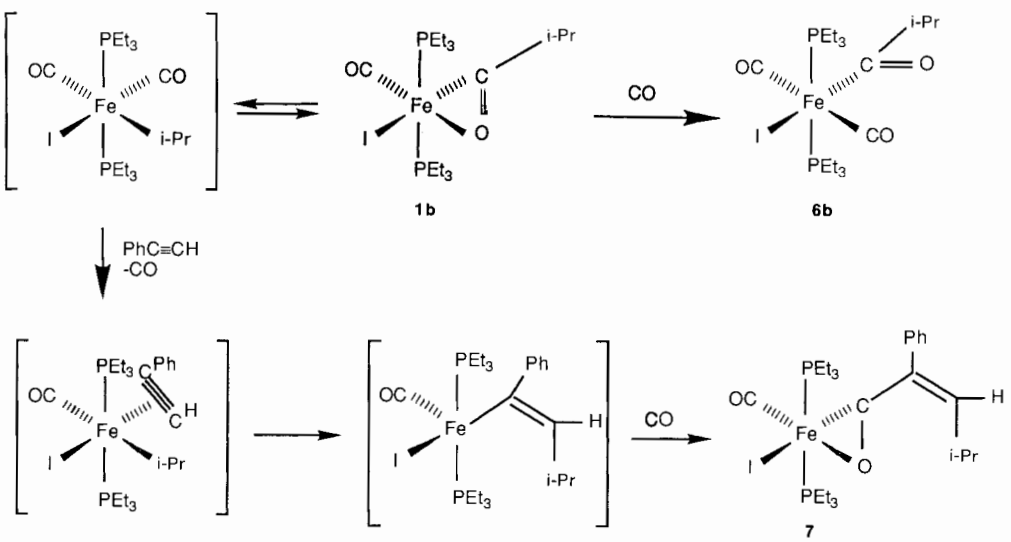

The reaction of **1b** with phenylacetylene produces a red crystalline (η^2-4-methyl-1-oxo-2-phenylpent-2-enyl)iron complex **7** in 37% yield whose structure was established by its ^{1}H- and ^{13}C-NMR data. Formation of **7** requires C–C bond cleavage in the isobutyryl group and probably occurs *via* an isopropyl intermediate, as indicated in *Scheme 2*.

The presence of an η^2-acyl unit in **7** is clearly shown by the chemical shift of the acyl C-atom and its coupling to the *cis* P-ligands (270.8 ppm, $J(^{13}C,^{31}P) = 34.5$ Hz; *Table 1*). The resonance of an η^1-acyl C-atom would be anticipated at some 20 ppm higher field. In comparison, the terminal carbonyl C-atom (C≡O) resonates at 224.1 ppm ($J(^{13}C,^{31}P) = 20.0$ Hz). The olefinic C-atoms in β- and γ-position relative to the Fe-center resonate at 136.7 and 164.3 ppm, respectively, and C(β) displays a 3-bond coupling to the P-nuclei ($J(^{13}C,^{31}P) = 2.3$ Hz). In the fully coupled ^{13}C-NMR spectrum, C(γ)-displays a ^1J(C,H) of 152 Hz to the olefinic proton. In addition, the η^2-acyl C-atom is coupled to the olefinic proton with a $^3J = 8.8$ Hz which suggests that these atoms lie in *trans*-positions with respect to the double bond. Finally, $(CH_3)_2CH$ is coupled to the olefinic-proton (J(H,H) = 10.7 Hz), confirming their proximity. Based on a comparison with structure **1a**, it is assumed that the O-atom of the η^2-acyl group of **7** is *cis* to the I-ligand.

Calculations. MEHT calculations [7] were carried out on model compounds to achieve further insight into the course of the migration reactions **2**→**3** and **2**→**5** (for parameters, see *Table 2*). Theoretical analyses of 1,2- and 1,3-acyl shifts are presently

Table 2. *Atomic Parameters Used in the MEHT and EHT Calculations*

Element	Orbital	H_{ii} [eV]	ζ_1	ζ_2	c_1	c_2
H	1s	–13.6	1.30			
C	2s	–21.4	1.625			
	2p	–11.4	1.625			
O	2s	–32.3	2.275			
	2p	–14.8	2.275			
P	3s	–18.5	1.600			
	3p	–14.0	1.600			
Fe	3d	–11.4	5.35	1.8	0.5366	0.6678
	4s	–9.1	1.40			
	4p	–3.52	1.40			

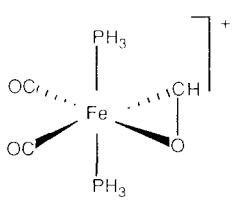

14

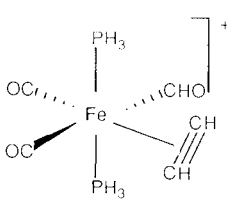

15

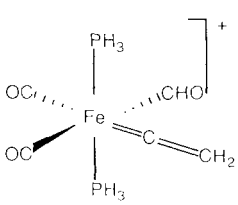

16

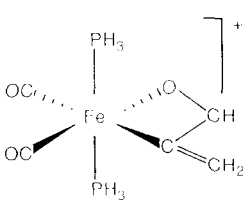

17

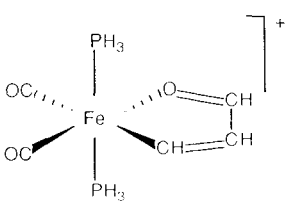

18

incomplete [1e] [8]. In this paper, potential-energy surfaces for these processes were computed in order to learn about characteristic electronic features of reaction courses and transition states of these elementary steps shown in *Scheme 1*.

Modelling of chemical reactivity by quantum-chemical methods always involves a simplified view when interpreting data in terms of thermodynamic parameters. Our analysis was started with extensive geometry optimizations on the model molecules **14**–**18**. The computed geometries of **14**–**18**, especially those parameters describing the coordination geometries around the Fe-centers were in good accord with expectations from related X-ray structural work [9] (for **15**–**18**, see *Tables 3* and *4*). The reliability of

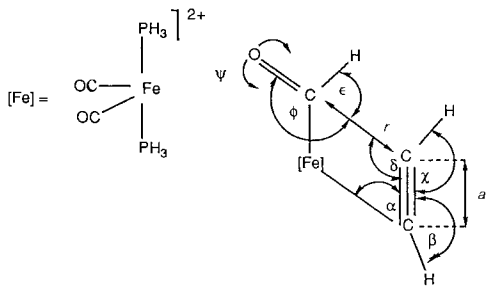

Table 3. *Variation of Geometrical Parameters of the Energy Hypersurface of* Fig. 2: *Optimized Values of Structures of* **15**, **19**, *and* **18**

	r [Å]	ϕ [°]	ψ [°]	a [Å]	α [°]	β [°]	χ [°]	δ [°]	ε [°]
15	2.60	174.7	0.0	1.30	72.9	167.5	170.2	118.8	72.6
19 (transition state)	2.00	129.5	80.0	1.35	78.2	163.5	144.9	123.9	108.2
18	1.61	115.2	0.0	1.45	110.5	125.6	129.2	107.2	126.7

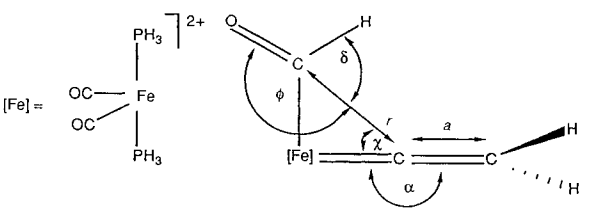

Table 4. *Variation of Geometrical Parameters of the Energy Hypersurface of* Fig. 5: *Optimized Values for the Structures of* **16**, **20**, *and* **17**

	r [Å]	ϕ [°]	a [Å]	α [°]	χ [°]	δ [°]
16	2.58	175.0	1.43	180.0	44.8	79.5
20 (transition state)	2.10	155.0	1.42	166.2	61.8	89.0
17	1.55	110.5	4.45	142.6	84.1	129.0

the calculations for **15** can be judged from the Fe–O and Fe–C(acyl) bond lengths of 2.6 and 1.87 Å, respectively. The metal-O separations in η^2-acyl complexes are represented by extremely flat potential energy curves. In view of this fact, the comparison of the above mentioned Fe–O and Fe–C bond lengths with the values of a related X-ray structure [5] of 2.19 and 1.80 Å suggest that the MEHT method can be confidently applied to our chemical problem.

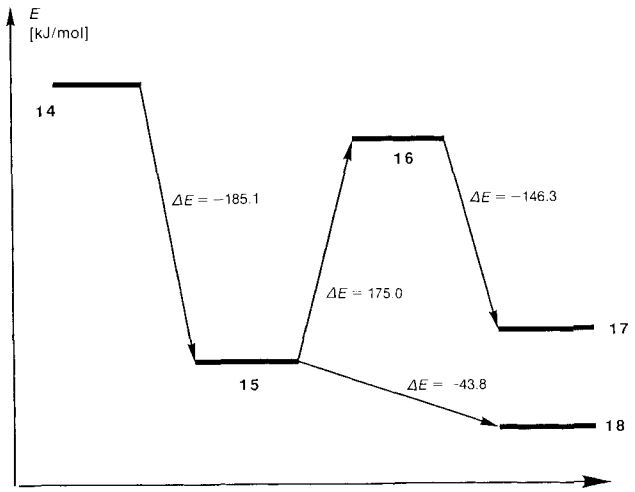

Fig. 1. *Potential-energy scheme of the reaction paths* **14**→**15**→**18** *and* **15**→**16**→**17**

According to *Fig. 1*, the coupling of an acetylene and a formyl unit at the Fe-center of a $[Fe(CO)_2(PH_3)_2]^{2+}$ moiety, *i.e.* the conversion **14**→**18** is found to be energetically downhill, while the transformation **14**→**17** is characterized by an energetic sink at **15** and a relatively high energetic barrier at **16**.

For the conversion **15**→**18**, a cut through the multidimensional energy hypersurface was established by varying two crucial parameters: the orientation of the formyl group (ψ) and the C(formyl)–C(acetylene) distance. As shown in *Table 3*, various other degrees of freedom were optimized at each point of the energy surface. The computed reaction path for the transformation **15**→**18** (*Fig. 2*) takes a smooth energetic uphill course to form the transition state **19** (geometrical parameters, see *Table 3*) at a saddle point 83.6

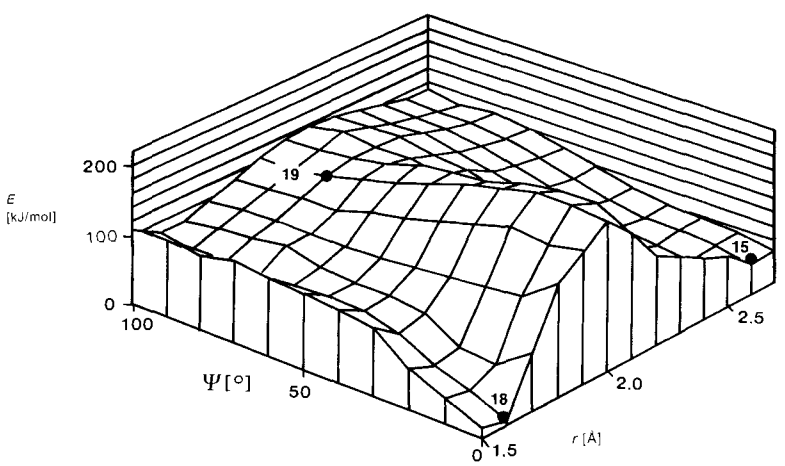

Fig. 2. *Computed energy-surface plot for the process* **15**→**18** via **19**. Degrees of freedom, see *Table 3*.

kJ/mol above **15**, in agreement with the limits from our experimental investigations. The most remarkable feature of **19** is that the formyl group adopts an almost upright position with respect to the plane of migration ($\psi = 80°$), because in the in-plane conformation the formyl O-atom is obviously exposed to repulsive interactions from the Fe-center. Continuing the travel to **18**, these forces become diminished and even attractive so that the formyl group is finally found orientated in-plane again. The least-energy pathway **15**→**18** *via* **19** does not correspond to a least-motion pathway.

The electronic features of the C–C bond forming process on going from **15** to **19** can be entirely understood by merely considering the coupling reaction of a formyl anion with an acetylene moiety. The in-plane interaction of the frontier orbitals of these units is shown in *Fig. 3* [10]. For the formyl group as a single-faced π-acceptor ligand, we expect a

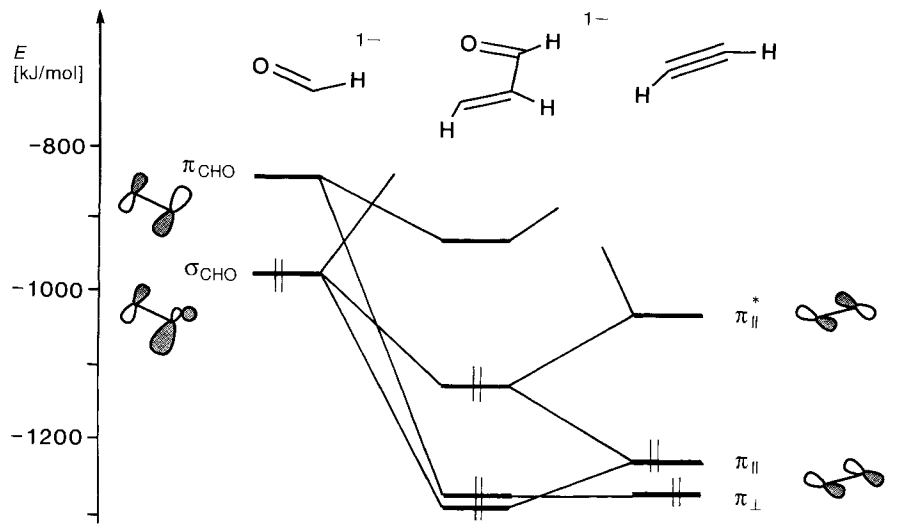

Fig. 3. *MO-Interaction scheme composing the frontier orbitals of a propenalide anion from formyl anion and acetylene wave functions*

relatively high lying σ-type formyl orbital in the HOMO/LUMO region [8] which is involved in a three-orbital interaction with π and π^* from the acetylene unit. The in-phase combination of σ_{formyl} and $\pi_{acetylene}$ represents primarily the newly formed internal σ C–C bond, while the expected nonbonding orbital consists of a mixture of all three starting functions, whereby π interacts out-of-phase and π^* in-phase with respect to the σ_{formyl} lobe. The resulting orbital is mainly of lone-pair character at the terminal C-atom of this organic residue. Adding a C_{2v} $[Fe(CO)_2(PH_3)_2]^{2+}$ fragment to the orbitals of CHO^- and acetylene of *Fig. 3* in the geometry of **15**, one obtains a quite conventional situation of orbital interactions, since we compose an 18 electron pseudooctahedral complex out of two two-electron-donating ligands and additional weak π-acceptor interactions and the orbitals of a d^6-FeL_4 residue. The MO scheme of complexes like **18** was theoretically analyzed earlier [1e]. In **18**, two more or less localized interactions of the enone system, the terminal C-atom and the energetically low-lying O-lone-pair functions utilize appropriate $[Fe(CO)_2(PH_3)_2]^{2+}$ fragment character.

To understand the specific geometrical arrangement of **19** with the formyl unit turned out of plane, it is best to look at a hypothetical molecule **19a** with the formyl group in plane. In **19a**, the evolving corresponding nonbonding orbital of *Fig. 3* does contain a considerable amount of antibonding interaction between the Fe and O wave functions. The partly generated terminal C-atom lone pair and the still existing σ_{formyl} character dominate the interaction to the Fe-center. As shown in *Fig. 4*, these lobes of the organic residue have to be in-phase with the orbitals of the Fe-center. Consequently, the O-function is then out-of-phase with respect to an adjacent orbital lobe of the Fe-center. This repulsive situation in the transition state can be prevented by an 80° rotation of the formyl unit as in **19**.

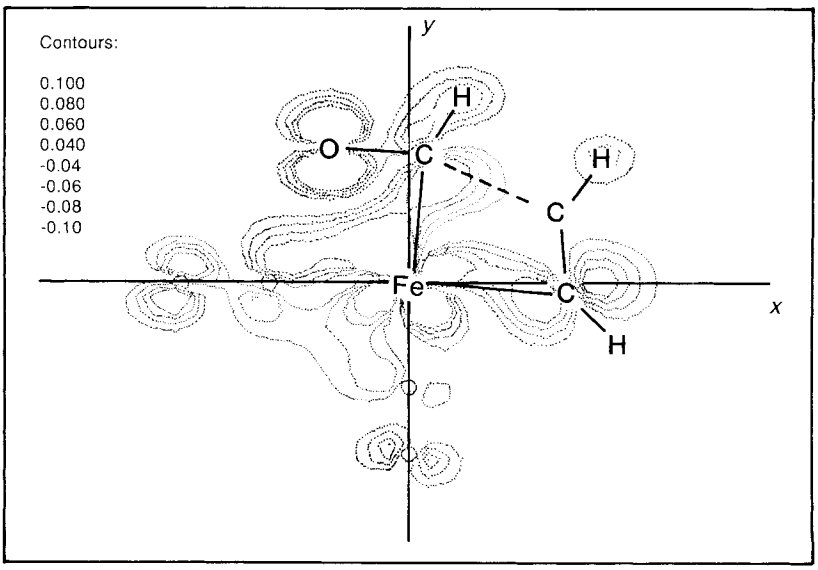

Fig. 4. *Wave-function contour plot of the HOMO in* **19a** *with the formyl and the acetylene unit in plane*

In order to explain the reaction path from **2a** to **5**, one should find support from calculations for the conversion **15** → **16** and the coupling **16** → **17**. In principle the acetylene/vinylidene rearrangement is a well known elementary step. Theoretical investigations suggest that this reaction should be quite feasible in general and that there are no obvious restrictions originating from the kind of transition-metal fragment [11]. We have, therefore, concentrated on computations of the metal-induced coupling of a formyl and an acetylene unit on going from **16** to **17**. *Fig. 5* represents a 2-dimensional slice through the energy hypersurface which was obtained by varying ϕ and r as indicated in *Table 4* and optimizing the residual degrees of freedom at each point of the surface. To proceed from **16**, one could follow a reaction path to the 'early' transition state **20** which would require 43.4 kJ/mol. From **16**, there is then a steady downhill slide to **17**. As indicated in *Scheme 1*, the formation of **5** can be accomplished either by a sequence of two elementary steps, an acetylene/vinylidene rearrangement and a subsequent coupling process of the

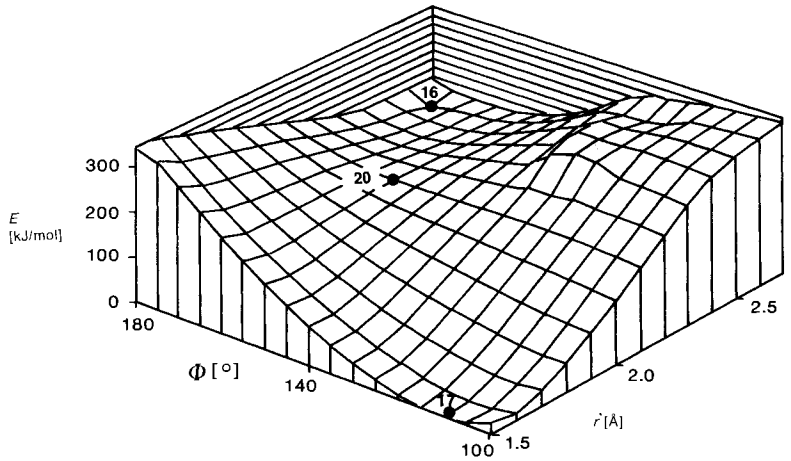

Fig. 5. *Computed energy-surface plot for the process* **16**→**17** via **20**. Degrees of freedom see *Table 4*.

acyl and the vinylidene unit, or a combination of both. Our model calculations on **15**–**17** have revealed that **16** lies at a relatively high thermodynamic level (see *Fig. 1*). This could on the one hand be caused by computational artifacts, but on the other hand it could indicate that **16** is not an intermediate of the conversion **15** → **17**. The electronic features of the process **16** → **17** are easily understood. They resemble the migration of an alkyl group to a metal-bound carbene unit which has been analyzed earlier [8b]. Unfortunately, it was not possible to pursue the combination of the acetylene rearrangement and the acyl/vinylidene coupling by computing a complete energy hypersurface, because of the too high dimensionality in the crucial degrees of freedom. But from the orbital pictures of the processes **15** → **16** and **16** → **17**, there is no indication of any restriction to a combined continuous transformation from **15** → **17**. Especially the circumstance that **20** would represent an early transition state in the process **16** → **17** and that the transformation **20** → **17** is extremely exothermic would suggest that an early attack of the formyl group during the reaction **15** → **16** would lead to an early stabilizing contribution in the combined conversion **15** → **17**.

It is quite remarkable to see that in **5** the Ph substituent is in the *cis*-position with respect to the Fe-center ((*Z*)-configuration). This regioselectivity again supports the existence of a combined reaction path on going from **2a** to **5**, because in this case there is no stereochemical pathway other than the attack of the acyl group on the same side of the C=C backbone as the H-atom migrates.

X-Ray Crystal Structure of **5**. Structural investigations on four-membered metallacylic complexes are quite rare [12]. They often have revealed unexpected features due to unusual electronic properties and the strain situation of the ring system. In order to gain further insight into the structural properties of this class of compounds and to establish a reference system for the discussed MO calculations, we carried out an X-ray structure analysis on **5**. Crystals suitable for this purpose were obtained by slowly cooling hexane solutions of **5** to −80°. Crystal, structure solution, and refinement data of **5** are given in *Table 5*.

Table 5. *Crystal, Structure Solution, and Refinement Data of* **5**

Empirical formula	$C_{24}H_{41}IFeO_2P_2$	Diffractometer	*Siemens R3m/V*
Color; habit	dark-blue prism	Radiation	Mo$K\alpha$ (λ = 0.71073 Å)
Crystal size [mm]	0.1 × 0.04 × 0.04	Temperature [K]	209
Crystal system	monoclinic	Monochromator	highly oriented graphite crystal
Space group	$P2_1/n$		
a [Å]	12.219(6)	2θ Range [°]	4.0–58.0
b [Å]	13.733(5)	Scan type	*Wyckoff*
c [Å]	16.519(6)	Scan speed	Variable; 1.50–15.00°/min in ω
β	99.88(3)°		
Volume [Å^3]	2731(2)	Scan range (ω)	1.20°
Z	4	Independent reflections	7306 (R_{int} = 13.61%)
Formula weight	606.3	Observed reflections	2579 ($F > 10.0\,\sigma(F)$)
Density (calc.) [mg/m^3]	1.475	Absorption correction	semi-empirical
Absorption coefficient [mm^{-1}]	1.803	Min./max. transmission	0.0131/0.0348
		Reflection 002 not used	
F(000)	1240	in least-squares calculations	
Solution	direct methods (*Siemens* SHELXTL PLUS; *Micro VAX II*)	R_F	8.87
		R_{F2}	6.65

From *Fig. 6* and *Table 6*, it can be seen that **5** has a pseudooctahedral coordination sphere around the transition-metal center. The Fe–O–C–C=C moiety is completely planar and exhibits only minor deviations from the expected values of distances and angles in C–C or C–O bonded systems (see *Table 6*).

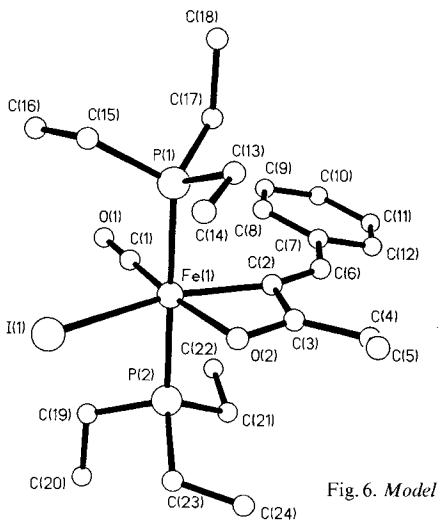

Fig. 6. *Model of the molecular structure of* **5**

Table 6. *Selected Bond Lengths* [Å] *and Angles* [°] *of* **5**

Fe(1)–C(2)	1.986 (14)	Fe(1)–C(2)–C(3)	89.8 (9)	Fe(1)–C(2)–C(6)	151.0 (11)
Fe(1)–O(2)	2.076 (9)	C(3)–C(2)–C(6)	118.9 (12)	C(2)–C(3)–O(2)	109.9 (11)
C(2)–C(6)	1.344 (22)	C(2)–C(3)–C(4)	128.5 (13)	O(2)–C(3)–C(4)	121.6 (13)
C(3)–C(4)	1.492 (19)	Fe(1)–O(2)–C(3)	93.0 (8)		
C(2)–C(3)	1.494 (19)	C(2)–C(6)–C(7)	134.1 (13)		
C(3)–O(2)	1.254 (18)	C(2)–Fe(1)–O(2)	67.3 (5)		

The Fe–C separation in the ring is somewhat longer than reference single bonds [9], which probably reflects the strain and the generally reduced bond strength in such cycles. The Fe–O(2) bond is longer than the Fe–C distance of the rings which is opposite to what would be predicted form the sum of covalent radii. The relatively loose coordination of the atom O(2) is accompanied by a somewhat shorter C(3)–O(2) distance. The transannular contact Fe–C(3) (2.481 Å) lies still in the range for a weak M–C interaction. This phenomenon is obviously a consequence of the geometric situation in the small ring. It is probably not governed by any sort of electronic driving forces. In principle, in closed-shell compounds such interactions of electronically saturated atoms should be repulsive as indicated by the MO calculations of **17**. In non-rare gas configured metallacyclobutadiene complexes, secondary transannular contacts are sometimes attractive and lead to significant distortions of the metallacyclic moiety.

We thank the *Swiss National Science Foundation* for financial support.

Experimental Part

General. All manipulations were performed under dry N_2. Solvents were dried and distilled under N_2 before use. Chromatographic separations were performed on 3 × 25 cm columns of silica gel *60 (Merck)* at −25°. Methyl prop-2-ynoate was obtained commercially and redistilled before use. Alkyl iodides and acetylenes were obtained commercially and used without further purification. FT-NMR: *Varian-Gemini 200* spectrometer. FT-IR: *Bio-Rad-FTS-45* instrument. MS: *Finnigan-MAT-8320* spectrometer.

Starting material [Fe(CO)$_3$(PEt$_3$)$_2$] was prepared according to a published procedure [13] with the following modifications: A soln. of PEt_3 (10 ml, 68.4 mmol) and $NaBH_4$ (0.87 g, 22.8 mmol) in BuOH (300 ml) was treated with pentacarbonyl iron (3.0 ml, 22.8 mmol) and stirred vigorously. After the initially vigorous gas evolution had subsided, the soln. was heated to reflux for 2 h. The solvent was then removed under vacuum and the residue washed with 50 ml of cold MeOH. The product was further dried under vacuum, then extracted into hexane. The hexane soln. was filtered over *Celite* and concentrated to the saturation point. Upon cooling to −30°, the product separated as white plates: 7.1 g (83%).

Complex [Fe(CO)$_2$(PEt$_3$)$_2$]$_2$N$_2$, carbonyliodo(η^2-propionyl)-trans-*bis(triethylphosphine)iron* (II) (**1a**) *and carbonyliodo(η^2-isobutyryl)*-trans-*bis(triethylphosphine)iron* (II) (**1b**) were prepared according to published procedures [6].

Reaction of **1a** *with Phenylacetylene.* A soln. of **1a** (1 g, 2 mmol) in Et_2O (150 ml) was treated with phenylacetylene (2.2 ml, 19.8 mmol) and heated to reflux for 100 h. The solvent was then removed unter partial vacuum and the residue chromatographed with Et_2O/hexane 1:3, yielding 3 bands. *Fraction 1* contained only paramagnetic side products. *Fraction 2* was chromatographed with hexane/CH_2Cl_2/AcOEt 8:1:1 and gave rise to 4 new zones. The 1st and 4th zones also contained only paramagnetic side products and the 2nd zone consisted of unreacted **1a**. The 3rd zone yielded *ca.* 50 mg (4%) of *carbonyliodo(3-oxo-1-phenylpent-1-enyl-*C^1,O*)*-trans-*bis(triethylphosphine)iron* (II) (**3**). The remaining *Fraction 3* from the first chromatography was dried under vacuum and extracted with hexane. The hexane extract was further chromatographed with hexane/CH_2Cl_2/AcOEt 8:1.5:0.5. The 1st zone contained 70 mg (5.8%) of *carbonyliodo(3-oxo-1-phenylpent-1-en-2-yl-*C^2,O*)*-trans-*bis(triethylphosphine)iron* (II) (**5**) which upon drying yielded a powdery blue solid. The 2nd zone consisted of *ca.* 30 mg (2.4%) of *dicarbonyliodo(3-oxo-1-phenylpent-1-enyl)*-trans-*bis(triethylphosphine)iron* (II) (**4**) and the 3rd zone contained *all*-trans-*dicarbonyliodo(propionyl)bis(triethylphosphine)iron* (II) (**6a**).

3: EI-MS: 578 ([*M* − CO]$^+$), 460 ([578 − PEt_3]$^+$), 419 ([578 − PhCHCOEt]$^+$), 301 ([419 − PEt_3]$^+$, [460 − CPhCHCOEt]$^+$), 292 ([419 − I]$^+$).

5: FAB-MS: 578 ([*M* − CO]$^+$), 460 ([578 − PEt_3]$^+$), 451 ([578 − I]$^+$), 419 ([578 − CPhCHCOEt]$^+$), 333 ([460 − I]$^+$, [451 − PEt_3]$^+$), 301 ([419 − PEt_3]$^+$, [460 − CPhCHCOEt]$^+$), 292 ([419 − I]$^+$).

Reaction of **1b** *with Phenylacetylene.* A soln. of **1b** (1.0 g, 1.93 mmol) in Et_2O (150 ml) was treated with phenylacetylene (2.1 ml, 19.0 mmol) and refluxed for 90 h. The solvent was removed under partial vacuum and the

residue chromatographed with hexane/CH_2Cl_2/AcOEt 8:1:1. Three bands were obtained, the second of which contained *carbonyliodo(4-methyl-1-oxo-2-phenylpent-2-enyl-*C^1,O)-trans-*bis(triethylphosphine)iron* (II) (**7**) and the third *all*-trans-*dicarbonyliodo(isobutyryl)bis(triethylphosphine)iron* (II) (**6b**). Compound **7** was recrystallized from hexane to yield 0.45 g (37%) of small red crystals. EI-MS: 592 ($[M - CO]^+$), 474 ($[592 - PEt_3]^+$), 419 ($[592 - PhCCH(i\text{-}Pr)]^+$), 301 ($[474 - PhCCH(i\text{-}Pr)]^+$), 292 ($[419 - I]^+$).

REFERENCES

[1] a) P. DeShong, G.A. Slough, *Organometallics* **1984,** *3,* 636; b) P. DeShong, G.A. Slough, V. Elango, G.L. Trainor, *J. Am. Chem. Soc.* **1985,** *107,* 778; c) P. DeShong, D.R. Sidler, G.A. Slough, *Tetrahedron Lett.* **1987,** *28,* 2233; d) P. DeShong, D.R. Sidler, P.J. Rybczynski, G.A. Slough, A.L. Rheingold, *J. Am. Chem. Soc.* **1988,** *110,* 2575; e) P. DeShong, D.R. Sidler, P.J. Rybczynski, G.A. Slough, W. v. Philipsborn, R.W. Kunz, B.E. Bursten, T.W. Clayton, Jr., *Organometallics* **1989,** *8,* 1381; f) L.S. Liebeskind, J.R. Gasdaska, J.S. McCallum, S.J. Tremont, *J. Org. Chem.* **1989,** *54,* 669; g) N.P. Robinson, L. Main, B.K. Nicholson, *J. Organomet. Chem.* **1989,** *364,* C37.

[2] H.G. Alt, G.S. Herrmann, H.E. Engelhardt, R.D. Rogers, *J. Organomet. Chem.* **1987,** *331,* 329; J.L. Davidson, M. Green, J.Z. Nyathi, C. Scott, F.G.A. Stone, A.J. Welch, P. Woodward, *J. Chem. Soc., Chem. Commun.* **1976,** 714; M. Bottrill, M. Green, *J. Chem. Soc., Dalton Trans.* **1979,** 820; C.A. Rusik, M.A. Collins, A.S. Gamble, T.L. Tonker, J.L. Templeton, *J. Am. Chem. Soc.* **1989,** *111,* 2550.

[3] J.R. Crook, B. Chamberlain, R.J. Mawby, *J. Chem. Soc., Dalton Trans.* **1989,** 465.

[4] E. Carmona, E. Gutièrez-Puebla, A. Monge, J.M. Marin, M. Paneque, M.L. Poveda, *Organometallics* **1989,** *8,* 967.

[5] R. Birk, H. Berke, G. Huttner, L. Zsolnai, *J. Organomet. Chem.* **1986,** *309,* C18.

[6] R. Birk, H. Berke, G. Huttner, L. Zsolnai, *Chem. Ber.* **1988,** *121,* 1557.

[7] A.B. Anderson, *J. Chem. Phys.* **1975,** *62,* 1187; D.A. Pensak, R.J. McKinney, *Inorg. Chem.* **1979,** *18,* 3407.

[8] H. Berke, R. Hoffmann, *J. Am. Chem. Soc.* **1978,** *100,* 7224.

[9] A.G. Orpen, L. Brammer, F.H. Allen, O. Kennard, D.G. Watson, R. Taylor, *J. Chem. Soc., Dalton Trans.* **1989,** S1.

[10] R. Hoffmann, *J. Chem. Phys.* **1963,** *39,* 1397; R. Hoffmann, W.N. Lipscomb, *ibid.* **1962,** *36,* 2179.

[11] J. Silvestre, R. Hoffmann, *Helv. Chim. Acta* **1985,** *68,* 1461.

[12] V.V. Ohjnik, P.Yu. Zawalii, M.G. Myskir, V.S. Fundamenskii, *Koord. Khim.* **1987,** *13,* 255; E. Delzado, J. Hein, J.C. Jeffery, A., L. Ratermann, F.G.A. Stone, L.J. Farrugien, *J. Chem. Soc., Dalton Trans* **1987,** 1191; E.D. Fischer, A.C. Filippo, H.G. Alt, U. Thewalt, *Angew. Chem. Int. Ed.* **1985,** *24,* 203; W.A. Herrmann, U. Kusthardt, A. Schafer, E. Herdtweck, *ibid.* **1986,** *25,* 817; E. Guggolz, M.L. Ziegler, H. Biersack, W.A. Herrmann, *J. Organomet. Chem.* **1980,** *194,* 317; R. Schlodder, J.A. Ibers, M. Lenarda, M. Graziani, *J. Am. Chem. Soc.* **1974,** *96,* 6893; G.A. Vaughan, G.L. Hillhouse, R.T. Lum, S.L. Buchwald, A.L. Rheingold, *ibid.* **1988,** *110,* 7215; M.R. Torres, A. Santos, J. Ros, X. Solans, *Organometallics* **1987,** *6,* 1091.

[13] R.L. Keiter, E.A. Keiter, K.H. Hecker, C.A. Boecker, *Organometallics* **1988,** *7,* 2466.